

## Differential excitation cross sections for electron impact on $\text{Li}^+$ : A study of continuum coupling effects

D. C. Griffin

*Department of Physics, Rollins College, Winter Park, Florida 32789  
and Physics Division, Oak Ridge National Laboratory, Oak Ridge, Tennessee 37831*

M. S. Pindzola

*Department of Physics, Auburn University, Auburn, Alabama 36849*

(Received 24 January 1990)

Differential excitation cross sections for the transitions from  $1^1S$  to  $2^3S$ ,  $2^1S$ ,  $2^3P$ , and  $2^1P$  in He-like  $\text{Li}^+$  are calculated in the distorted-wave and close-coupling approximations in order to study their sensitivity to continuum coupling effects. Comparisons are made between nonunitarized distorted-wave, 5-state unitarized distorted-wave, 5-state close-coupling, and 11-state close-coupling calculations. The results indicate that the shape of the cross sections, as a function of scattering angle, can be significantly different for the various levels of approximation, even when the total cross sections are in reasonably close agreement.

### I. INTRODUCTION

Although many calculations and measurements of differential cross sections have been made for electron impact with neutral atoms (see, for example, Ref. 1), little work has been done on differential cross sections for electron-ion collisions, mainly because of the lack of any experimental data. However, relative measurements of differential cross sections over a limited range of angles have been made,<sup>2</sup> and it appears that measurements of partial cross sections over a range of scattering angles may now be possible with a new generation of electron-ion scattering experiments.<sup>3</sup> For this reason, we have made a series of differential excitation cross-section calculations to investigate the sensitivity of such cross sections to various levels of scattering approximation.

We have performed distorted-wave and close-coupling calculations for the  $1^1S \rightarrow 2^3S$ ,  $1^1S \rightarrow 2^1S$ ,  $1^1S \rightarrow 2^3P$ , and  $1^1S \rightarrow 2^1P$  excitations in He-like  $\text{Li}^+$ . This particular ion was chosen since close-coupling calculations<sup>4,5</sup> of the total cross sections for all the above transitions have been reported, a measurement of the total cross section for the  $1^1S \rightarrow 2^3P$  excitation has been made,<sup>6</sup> and

differential cross-section calculations using a nonunitarized distorted-wave approximation have been performed.<sup>7,8</sup> In the present study, we compare differential excitation cross sections for  $\text{Li}^+$  calculated in nonunitarized distorted-wave, 5-state unitarized distorted-wave, 5-state close-coupling, and 11-state close-coupling approximations. These results should provide an indication of the sensitivity of electron-ion differential cross sections to the details of the scattering approximation.

The remainder of this paper is arranged as follows. In Sec. II we give a brief summary of the theory of differential electron-impact cross sections for ions, and discuss the computational methods that we have employed. In Sec. III the results of our various calculations are presented and compared with each other and with prior work. Finally, in Sec. IV, we provide a brief summary of the calculations and discuss their implications.

### II. THEORETICAL METHODS

The scattering amplitude for electron-ion scattering from an initial state  $\alpha_i L_i S_i M_{L_i} M_{S_i}$  to a final state  $\alpha_f L_f S_f M_{L_f} M_{S_f}$  in  $LS$  coupling is given by

$$f_{fi}(\theta, \phi) = \left[ \frac{(q/k_i) \delta_{\alpha_i \alpha_f} \delta_{L_i L_f} \delta_{M_{L_i} M_{L_f}} \delta_{S_i S_f} \delta_{M_{S_i} M_{S_f}} \delta_{m_i m_f}}{2k_i \sin^2(\theta/2)} e^{i2\sigma_0} e^{i(q/k_i) \ln[\sin^2(\theta/2)]} \right] + \left[ i(\pi/k_i k_f)^{1/2} \sum_{\substack{l_i, l_f, m_i, m_f \\ L, S, \Pi, M_L, M_S}} i^{(l_i - l_f)} (2l_i + 1)^{1/2} e^{i(\sigma_{l_i} + \sigma_{l_f})} C_{M_{L_i} 0 M_L}^{L_i l_i L} C_{M_{S_i} m_i M_S}^{S_i 1/2 S} \times C_{M_{L_f} l_f M_L}^{L_f l_f L} C_{M_{S_f} m_f M_S}^{S_f 1/2 S} T_{l_i l_f}^{LS\Pi}(\beta_i \rightarrow \beta_f) Y_{l_f m_f}(\theta, \phi) \right], \quad (1)$$

where the first term in large parentheses represents purely Coulombic scattering in the elastic channel;  $q$  is the charge of the ion;  $k_i$  and  $k_f$  are the linear momenta of the incident and scattered electrons, respectively;  $l_i$ ,  $m_{l_i}$ , and  $m_i$ , and  $l_f$ ,  $m_{l_f}$ , and  $m_f$  are the orbital angular momentum, orbital magnetic, and spin magnetic quantum numbers of the incident and scattered electrons, respectively;  $\sigma_l$  is the Coulomb phase shift;  $\beta$  is used to represent the quantum numbers  $\alpha LS$  specifying the initial and final terms in  $LS$  coupling; the symbol  $C$  is used to signify the Clebsch-Gordan coefficients;  $T_{l_i l_f}^{LS\Pi}(\beta_i \rightarrow \beta_f)$  is an element of the  $\underline{T}$  matrix for a given total angular momentum  $L$ , total spin  $S$ , and parity  $\Pi$ , connecting the channel  $\beta_i l_i$  with the channel  $\beta_f l_f$ ; and the  $\underline{T}$  matrix is related to the  $\underline{S}$  matrix and the  $\underline{R}$  matrix by the equation

$$\begin{aligned} \frac{d\sigma_{if}}{d\Omega} = & \frac{(q/k_i)^2 \delta_{\beta_i \beta_f}}{4k_i^2 \sin^4(\theta/2)} - \frac{(q/k_i) \delta_{\beta_i \beta_f}}{4(2L_i+1)(2S_i+1)k_i^2 \sin^2(\theta/2)} \\ & \times \text{Im} \left[ e^{-i(q/k_i) \ln[\sin^2(\theta/2)]} \sum_{l_i, L, S, \Pi} e^{i2(\sigma_{l_i} - \sigma_0)} (2L+1)(2S+1) T_{l_i l_i}^{LS\Pi}(\beta_i \rightarrow \beta_i) P_{l_i}(\cos\theta) \right] \\ & + \frac{1}{8(2L_i+1)(2S_i+1)k_i^2} \sum_{\lambda} (2\lambda+1) \left[ \sum_{l_i, l_i, \bar{l}_i, \bar{l}_f} \begin{Bmatrix} l_i & \bar{l}_i & \lambda \\ 0 & 0 & 0 \end{Bmatrix} \begin{Bmatrix} l_f & \bar{l}_f & \lambda \\ 0 & 0 & 0 \end{Bmatrix} i^{(l_i - l_f)(\bar{l}_f - \bar{l}_i)} e^{i(\sigma_{l_i} - \sigma_{\bar{l}_i} + \sigma_{l_f} - \sigma_{\bar{l}_f})} \right. \\ & \times \sum_{j_i} (-1)^{j_i + \lambda} (2j_i + 1) \begin{Bmatrix} l_i & l_f & j_i \\ \bar{l}_i & \bar{l}_f & \lambda \end{Bmatrix} \\ & \left. \times \sum_S M^*(\beta_i \bar{l}_i \beta_f \bar{l}_f j_i S) M(\beta_i l_i \beta_f l_f j_i S) \right] P_{\lambda}(\cos\theta), \quad (4) \end{aligned}$$

where the first two terms occur only in the elastic channel,  $j_i$  is the momentum-transfer quantum number employed by Salvini,<sup>9</sup> and  $M(\beta_i l_i \beta_f l_f j_i S)$  is defined by the equation

$$M(\beta_i l_i \beta_f l_f j_i S) = \sum_{\Pi, L} (-1)^{l_i + l_f} [(2L_i+1)(2L_f+1)(2S+1)]^{1/2} (-1)^L (2L+1) \begin{Bmatrix} L_i & L_f & j_i \\ l_f & l_i & L \end{Bmatrix} T_{l_i l_f}^{LS\Pi}(\beta_i \rightarrow \beta_f), \quad (5)$$

which is within a phase factor of Salvini's definition of  $M$ .<sup>9</sup>

We have written a program similar to Salvini's MOMTRANF code<sup>9</sup> that calculates differential cross sections using Eqs. (4) and (5). The program reads  $\underline{R}$  matrices or  $\underline{T}$  matrices from a distorted-wave or close-coupling calculation and generates total and differential cross sections and plots of differential cross sections as a function of the scattering angle  $\theta$ .

For the results presented here, all orbitals were generated using Fischer's Hartree-Fock (HF) program.<sup>10</sup> The  $1s$  orbital was obtained from a Hartree-Fock calculation of  $\text{Li}^+ 1s^2$ . The  $2s$ ,  $2p$ ,  $3s$ ,  $3p$ , and  $3d$  orbitals were obtained from frozen-core Hartree-Fock calculations for the appropriate  $1snl$  configuration.

The nonunitarized distorted-wave (DW) and the 5-state unitarized distorted-wave (UDW) calculations were performed with our distorted-wave code for which the continuum electrons are determined in a full Hartree-Fock

$$\underline{T} = \underline{1} - \underline{S} = - \frac{2i\underline{R}}{(\underline{1} - i\underline{R})}. \quad (2)$$

The differential cross section is then determined by squaring the scattering amplitude, averaging over the initial states, summing over the final states, and multiplying by the ratio of the final to the initial linear momenta:

$$\begin{aligned} \frac{d\sigma_{if}}{d\Omega} = & \frac{1}{2(2L_i+1)(2S_i+1)} \frac{k_f}{k_i} \\ & \times \sum_{\substack{M_{L_i}, M_{L_f}, M_{S_i} \\ M_{S_f}, m_i, m_f}} |f_{fi}(\theta, \phi)|^2. \quad (3) \end{aligned}$$

After some Racah algebra, one obtains the equation for the differential cross section in atomic units per steradian (a.u./sr) as

potential. In these calculations, we did not force orthogonality between the continuum and bound orbitals with the same angular symmetry, but rather included the exchange overlap terms within the distorted-wave potential.<sup>11</sup> The close-coupling (CC) calculations were performed using the IMPACT code of Crees *et al.*<sup>12</sup>

The configuration-interaction (CI) target states and angular algebra for the distorted-wave and close-coupling calculations were generated using the program COLALG.<sup>13</sup> The COLALG output files were modified for the distorted-wave calculation to exclude all coefficients associated with bound channels and add the coefficients for the exchange-overlap terms. For the DW, the 5-state UDW and the 5-state close-coupling (CC5) calculations, the CI target states were obtained by mixing the even-parity configurations  $1s^2$ ,  $1s2s$ ,  $2s^2$ , and  $2p^2$ , and the odd parity configurations  $1s2p$  and  $2s2p$ ; however,  $2s^2$ ,  $2s2p$ , and  $2p^2$  were treated as correlation configurations, and only the five terms arising from  $1s^2$ ,  $1s2s$ , and  $1s2p$  were in-

cluded within the  $\underline{R}$  matrix for the UDW calculation and within the coupled equations of the CC5 calculation. For the 11-state close-coupling (CC11) calculations, the target states were generated from the even parity configurations  $1s^2$ ,  $1s2s$ ,  $1s3s$ ,  $1s3d$ ,  $2s^2$ , and  $2p^2$ , and the odd configurations  $1s2p$ ,  $1s3p$ , and  $2s2p$ , with  $2s^2$ ,  $2s2p$ , and  $2p^2$  again being treated as correlation configurations only.

All calculations presented here were made for partial waves from  $L=0$  up to a maximum  $L$ ,  $L_{\max}$ , of 20. In order to test for convergence, we compared differential cross sections for different values of  $L_{\max}$  at an energy of 9.0 Ry, which was the highest electron energy employed. We found that the spin-changing transitions  $1^1S \rightarrow 2^3S$  and  $1^1S \rightarrow 2^3P$  have converged with  $L_{\max}=10$ . The spin-allowed transitions converge more slowly; however, the  $1^1S \rightarrow 2^1S$  transition has easily converged with a value of  $L_{\max}$  of 15, while the dipole-allowed transition  $1^1S \rightarrow 2^1P$  has converged with  $L_{\max}=18$ . Of course, for higher electron energies, higher partial waves would be required.

### III. RESULTS

In Table I we present theoretical energies for excitation from the  $1^1S$  ground-state term to the  $2^3S$ ,  $2^1S$ ,  $2^3P$ , and  $2^1P$  terms for  $\text{Li}^+$ , calculated using the two CI target states mentioned in Sec. II, in comparison to the corresponding experimental excitation energies.<sup>14</sup> The largest improvement of these energies over the corresponding single-configuration HF energies comes from configuration interaction with the correlation configurations  $2s^2$ ,  $2s2p$ , and  $2p^2$ . Also shown are the theoretical energies calculated by Christensen and Norcross<sup>5</sup> using their target model 3; this model was chosen for comparison because, of the targets which they employed in their calculations, it most closely resembles our choice of target states. Their energies are in somewhat better agreement with experiment than ours because they optimized their radial functions to improve the energies, rather than using single-configuration HF orbitals within a CI calculation.

In Table II we compare total excitation cross sections determined from our DW, UDW, CC5, and CC11 calculations at energies of 5.2 and 9.0 Ry. Also shown are approximate values of the total cross sections for  $1^1S \rightarrow 2^3S$  transition at an energy of 5.2 Ry and the  $1^1S \rightarrow 2^3P$  tran-

TABLE II. Excitation cross sections ( $10^{-2}$  a.u.).

Transition	DW <sup>a</sup>	DW <sup>b</sup>	UDW <sup>c</sup>	CC5 <sup>d</sup>	CC11 <sup>e</sup>
Electron energy = 5.2 Ry					
$1^1S-2^3S$	4.8	1.389	1.417	3.282	2.427
$1^1S-2^1S$		5.945	5.274	4.450	2.910
$1^1S-2^3P$		11.240	9.944	7.718	5.128
$1^1S-2^1P$		8.776	7.663	6.985	4.324
Electron energy = 9.0 Ry					
$1^1S-2^3S$		0.523	0.493	0.597	0.617
$1^1S-2^1S$		4.097	4.065	2.873	2.479
$1^1S-2^3P$	2.6	2.619	2.537	2.212	2.287
$1^1S-2^1P$		12.716	12.199	12.014	10.621

<sup>a</sup>Nonunitarized distorted wave, Itikawa and Sakimoto, Ref. 7, determined by integrating their differential cross sections.

<sup>b</sup>Nonunitarized distorted wave, this work.

<sup>c</sup>5-state unitarized distorted wave, this work.

<sup>d</sup>5-state close coupling, this work.

<sup>e</sup>11-state close coupling, this work.

sition at an energy of 9.0 Ry from the nonunitarized distorted-wave calculations of Itikawa and Sakimoto.<sup>7</sup> These were determined by numerically integrating the differential cross sections taken from the curves in their paper over the solid angle. The total cross section from their DW calculation for the  $1^1S \rightarrow 2^3P$  transition at an energy of 9.0 Ry is in excellent agreement with our DW calculation. However, their DW value for the  $1^1S \rightarrow 2^3S$  transition at an energy of 5.2 Ry is seen to be about 3.5 times our DW value. We investigated the sensitivity of this particular cross section to the distorting potential; however, we found only small variations in the total cross section, and therefore are unable to explain the large difference between the results from these two calculations. Sakimoto and Itikawa have also made differential cross section calculations for the  $1^1S \rightarrow 2^1S$  and  $1^1S \rightarrow 2^1P$  excitations,<sup>8</sup> but they were done at different electron energies and their results are, therefore, not included here.

We also notice from this table that coupling with the  $1s3l$  configurations, included in the CC11 calculation, has a rather significant effect on the total cross section, especially at the lower energy. This may indicate that coupling with the  $1s4l$  configurations is also important.

TABLE I. Excitation energies (in Ry).

Transition	Target 1 <sup>a</sup>	Target 2 <sup>b</sup>	Target 3 <sup>c</sup>	Experimental <sup>d</sup>
$1^1S-2^3S$	4.332	4.330	4.344	4.338
$1^1S-2^1S$	4.471	4.467	4.476	4.478
$1^1S-2^3P$	4.486	4.485	4.503	4.504
$1^1S-2^1P$	4.573	4.572	4.579	4.573

<sup>a</sup>Target 1.  $^1S$ ,  $1s^2+1s2s+2s^2+2p^2$ ;  $^3S$ ,  $1s2s$ ;  $^{1,3}P$ ,  $1s2p+2s2p$ ; with HF frozen-core orbitals, this work.

<sup>b</sup>Target 2.  $^1S$ ,  $1s^2+1s2s+1s3s+2s^2+2p^2$ ;  $^3S$ ,  $1s2s+1s3s$ ;  $^{1,3}P$ ,  $1s2p+1s3p+2s2p$ ; with HF frozen-core orbitals, this work.

<sup>c</sup>Target 3. Target model 3, of Christensen and Norcross, Ref. 5.

<sup>d</sup>Experimental energies from Ref. 14.

TABLE III. Comparison of close-coupling total cross sections in units of  $10^{-19}$  cm<sup>2</sup> at an energy of 5.2 Ry.

Transition	CC5 <sup>a</sup>	CC5 <sup>b</sup>	CC5 <sup>c</sup>	CC11 <sup>d</sup>	Expt. <sup>e</sup>
$1^1S-2^3S$	9.2	7.8	9.2	6.8	
$1^1S-2^1S$	12.4	7.2	12.5	8.1	
$1^1S-2^3P$	21.1	19.1	21.6	14.4	15.6
$1^1S-2^1P$	18.9	17.8	19.6	12.1	

<sup>a</sup>5-state close coupling, Wyngaarden, Bhadra, and Henry, Ref. 4.

<sup>b</sup>5-state close coupling, Christensen and Norcross, Ref. 5, using their target model 3.

<sup>c</sup>5-state close coupling, this work.

<sup>d</sup>11-state close coupling, this work.

<sup>e</sup>Experimental value, Rogers, Oslon, and Dunn, Ref. 6, at an energy of 5.23 Ry.

However, in the case of neutral He, comparison of the total collision strengths calculated from 5-state,<sup>15</sup> 11-state,<sup>16</sup> and 19-state<sup>17</sup>  $R$ -matrix calculations for the  $1^1S \rightarrow 2^3P$  transition indicate that only a small additional improvement is obtained by including the  $1s4l$  states in a 19-state calculation.

In Table III we compare our CC calculations of the total cross sections at an energy of 5.2 Ry with the CC5 calculations of Wyngaarden *et al.*<sup>4</sup> and those of Christensen and Norcross using their target model 3 (Ref. 5). As can be seen, our CC5 results are in good agreement with those of Wyngaarden *et al.*,<sup>4</sup> but the CC5 results of Christensen and Norcross<sup>5</sup> are significantly lower. These lower cross sections are presumably due to the better tar-

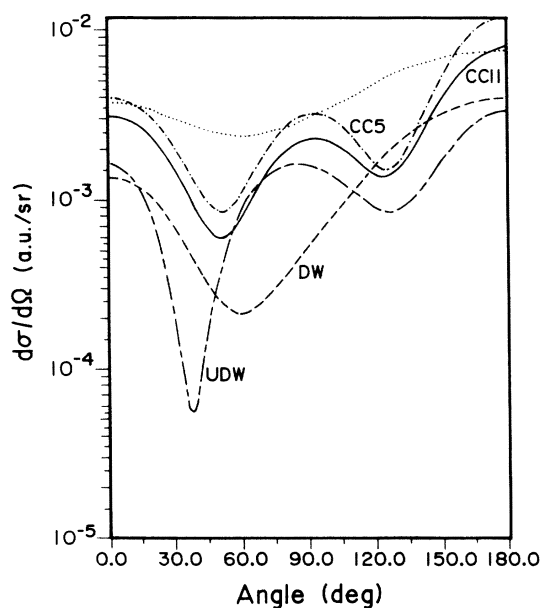


FIG. 1. Differential cross section  $d\sigma/d\Omega$  in units of a.u./sr for the  $1^1S \rightarrow 2^3S$  transition in  $\text{Li}^+$  at an energy of 5.2 Ry. Dotted curve, DW calculation of Itikawa and Sakimoto, Ref. 7; dashed curve, DW calculation, this work; long-dashed-short-dashed curve, UDW calculation; dot-dashed curve, CC5 calculation; solid curve, CC11 calculation.

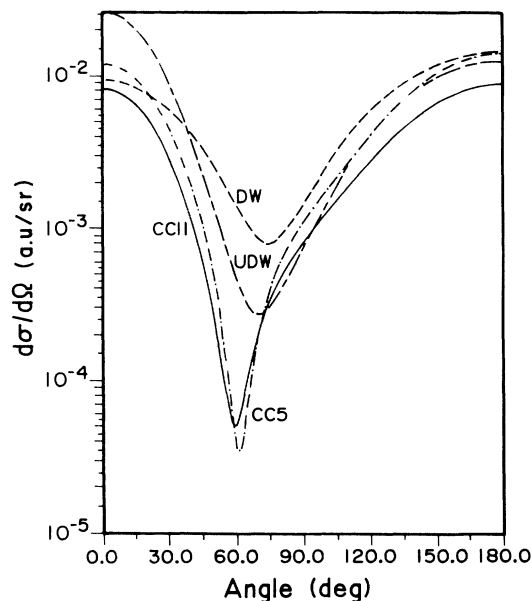


FIG. 2. Differential cross section for the  $1^1S \rightarrow 2^1S$  transition in  $\text{Li}^+$  at an energy of 5.2 eV. Dashed curve, DW calculation; long-dashed-short-dashed curve, UDW calculation; dot-dashed curve, CC5 calculation; solid curve, CC11 calculation.

get states that were employed in their calculations. Also shown in this table is the experimental total cross section of Rogers *et al.*<sup>6</sup> for the  $1^1S \rightarrow 2^3P$  transition at an energy of 5.23 Ry. Our CC11 cross section for this transition is in the best agreement with this value, although still nearly 8% lower.

Plots of our DW, UDW, CC5, and CC11 differential cross sections for these  $1s \rightarrow 2l$  transitions at an energy of 5.2 Ry are shown in Figs. 1–4, and for an energy of 9.0

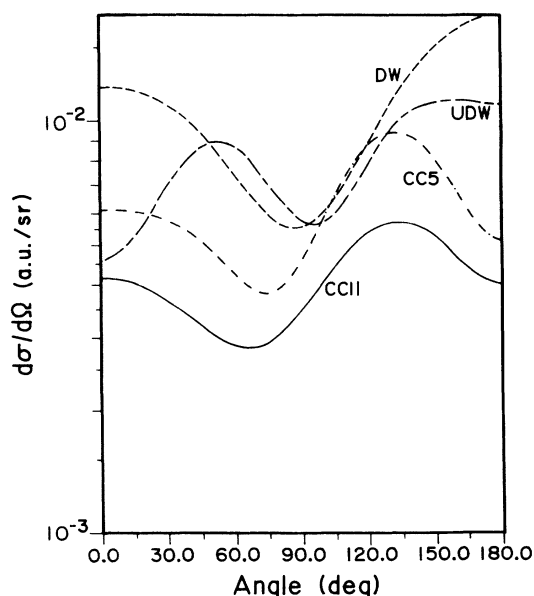


FIG. 3. Differential cross section for the  $1^1S \rightarrow 2^3P$  transition in  $\text{Li}^+$  at an energy of 5.2 Ry. Same notation as in Fig. 2.

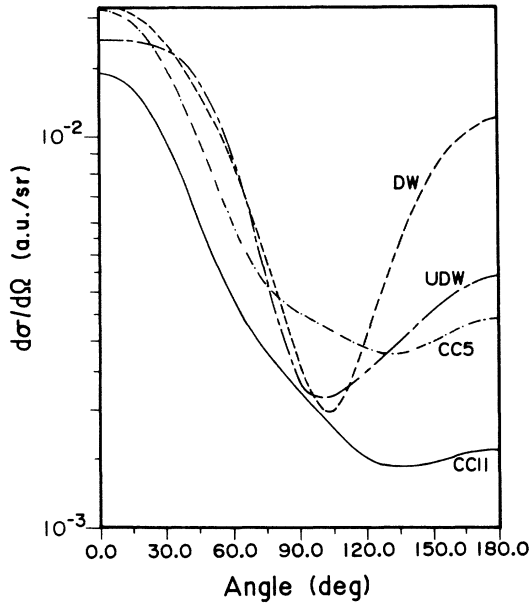


FIG. 4. Differential cross section for the  $1^1S \rightarrow 2^1P$  transition in  $\text{Li}^+$  at an energy of 5.2 Ry. Same notation as in Fig. 2.

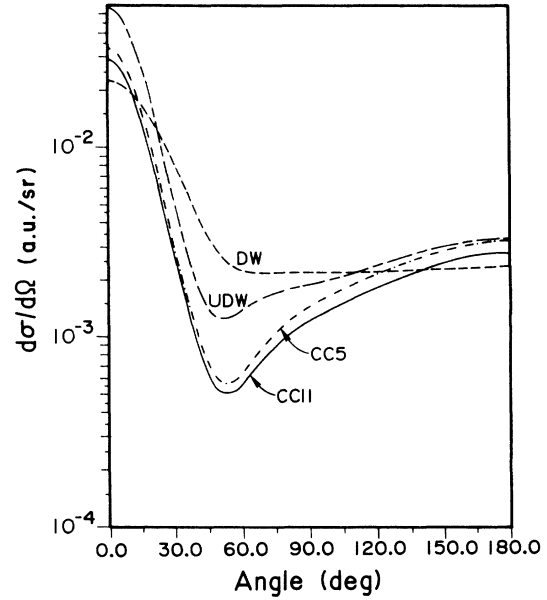


FIG. 6. Differential cross section for the  $1^1S \rightarrow 2^1S$  transition in  $\text{Li}^+$  at an energy of 9.0 Ry. Same notation as in Fig. 2.

Ry in Figs. 5–8. For comparison, we also show the DW differential cross section of Itikawa and Sakimoto<sup>7</sup> for the  $1^1S \rightarrow 2^3S$  transition in Fig. 1, and their DW differential cross section for the  $1^1S \rightarrow 2^3P$  transition in Fig. 7. It is not possible to make any general statements regarding the shape of these cross sections as a function of scattering angle because of the complex quantum-mechanical interference effects that occur at various angles. However, a comparison of these curves calculated at different levels of approximation does reveal the extreme sensitivity of differential cross sections to continuum coupling effects.

As can be seen, the DW and CC differential cross sections are significantly different, not only in magnitude, but also with respect to their variation as a function of the scattering angle. This is particularly true of the  $1^1S \rightarrow 2^3S$  and  $1^1S \rightarrow 2^3P$  spin-changing transitions at an energy of 5.2 Ry shown in Figs. 1 and 3. These cross sections are dominated by low partial waves (especially the  $1^1S \rightarrow 2^3S$  excitation), and in the DW approximation, are only possible through the exchange interaction. The DW curves are smooth, have a single minimum below  $90^\circ$ , and large backward-scattering contributions. However, the

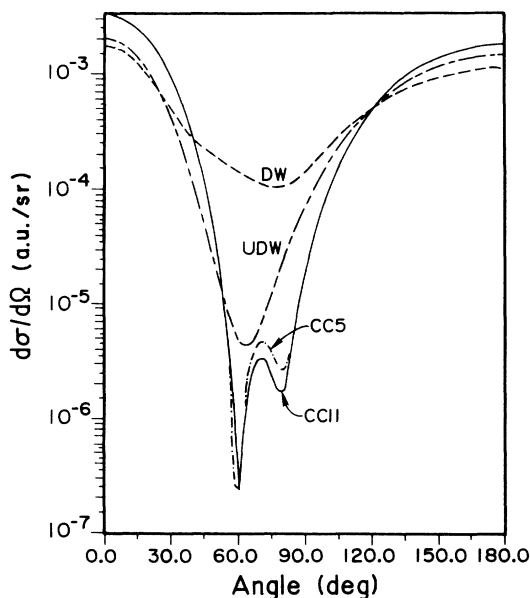


FIG. 5. Differential cross section for the  $1^1S \rightarrow 2^3S$  transition in  $\text{Li}^+$  at an energy of 9.0 Ry. Same notation as in Fig. 2.

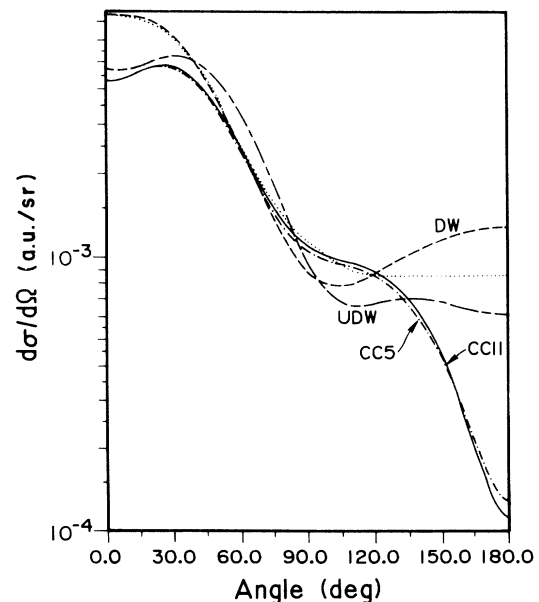


FIG. 7. Differential cross section for the  $1^1S \rightarrow 2^3P$  transition in  $\text{Li}^+$  at an energy of 9.0 Ry. Same notation as in Fig. 1.

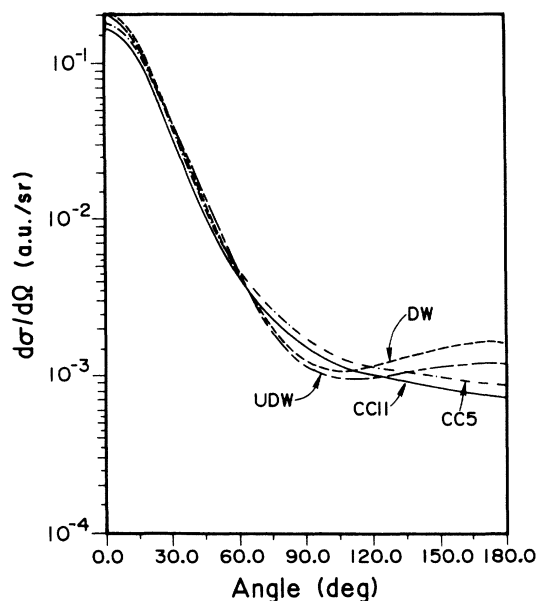


FIG. 8. Differential cross section for the  $1^1S \rightarrow 2^1P$  transition in  $\text{Li}^+$  at an energy of 9.0 Ry. Same notation as in Fig. 2.

continuum coupling included in the CC5 and CC11 calculations causes much more complex interference effects as a function of scattering angle. In fact, the CC calculations show two distinct minima for the  $1^1S \rightarrow 2^3S$  transition and a pronounced decrease in the large-angle backward-scattering cross section in the case of the  $1^1S \rightarrow 2^3P$  transition. It is also interesting to note how the limited coupling included within the UDW approximation also reflects this more complex angular dependence.

At the higher energy of 9.0 Ry, the differences in shape between the DW and CC calculations for the spin-changing transitions (Figs. 5 and 7) are somewhat less pronounced, although still much larger than one would expect on the basis of the relatively small differences in the total cross sections. In the case of the transition to the  $2^3S$  term, continuum coupling effects cause a much larger decrease in the cross section at intermediate angles and two distinct minima persist in both close-coupling calculations. For the  $1^1S \rightarrow 2^3P$  excitation, the four curves have similar shapes for scattering angles less than  $90^\circ$ , but the strong coupling included in the CC5 and CC11 calculations causes a marked decrease in the large-angle backward-scattering cross section; this effect is only weakly reflected by the limited coupling included in the UDW approximation.

The complex variations of the CC differential cross sections with scattering angle are much less severe for the spin-allowed excitations to  $2^1S$  and  $2^1P$ . In the case of the  $1^1S \rightarrow 2^1S$  excitation, the CC calculations have a much deeper minimum than the DW calculation at an energy of 5.2 Ry (Fig. 2), but this difference is less pronounced at the higher energy (Fig. 6). For the dipole-allowed transition  $1^1S \rightarrow 2^1P$  at 5.2 Ry (Fig. 4), the CC cross sections are quite different from the DW result, especially at large angles; however, at an energy of 9.0 Ry

(approximately twice the threshold energy), the curves are beginning to converge, especially for small scattering angles (see Fig. 8). The better agreement in this case is due to the fact that the cross sections for the dipole-allowed transitions, especially for higher electron energies and smaller scattering angles, are much more dependent on high partial waves, which are not nearly as sensitive to continuum coupling.

Although there are some significant differences between the magnitudes of the cross sections from the CC5 and CC11 calculations at the lower energy of 5.2 Ry, it is interesting to note that, for all transitions, there is good overall agreement with respect to the shape of these cross sections. This seems to indicate that the most important coupling effects have been included within the 5-state calculation. It is also important to observe that for all transitions, the variation in the shape of the cross sections with energy is large and unpredictable, especially for the two CC calculations, and it is most pronounced for the spin-changing  $1^1S \rightarrow 2^3S$  and  $1^1S \rightarrow 2^3P$  transitions (compare Fig. 1 with Fig. 5 and Fig. 3 with Fig. 7). This would make any interpolation of the differential cross sections as a function of energy virtually impossible.

The differential cross sections are also sensitive to the details of the calculation within the DW approximation. From Fig. 1, we see that our DW calculation of the differential cross section for the transition  $1^1S \rightarrow 2^3S$  at 5.2 Ry is significantly lower than that of Itikawa and Sakimoto,<sup>7</sup> as one would expect from a comparison of the total cross sections. However, from Fig. 7, we see that our DW calculation for the  $1^1S \rightarrow 2^3P$  transition at 9.0 Ry has a somewhat different shape than that of Itikawa and Sakimoto,<sup>7</sup> especially for the larger scattering angles, even though the total cross sections appear to be in good agreement. Finally, Sakimoto and Itikawa<sup>8</sup> have also performed a calculation for the  $1^1S \rightarrow 2^1P$  transition at an energy of about 9.15 Ry. Their differential cross section appears to have a shape similar to that obtained from our DW calculation and is in close agreement with our DW cross section for small scattering angles; however, their cross section is about 56% of our DW result for a scattering angle of  $180^\circ$ .

Finally, it is interesting to note that the variations of the differential cross sections with scattering angle determined from our CC calculations for  $\text{Li}^+$  at 5.2 Ry are similar for all transitions to those determined from a 19-state  $R$ -matrix calculation for neutral He by Fon *et al.*<sup>1</sup> This is true even though their calculation was performed at an energy 1.5 times the threshold for the  $1^1S \rightarrow 2^3S$  transition, while 5.2 Ry corresponds to about 1.2 times this threshold in  $\text{Li}^+$ . These similarities in the  $\text{Li}^+$  and neutral He calculations are somewhat surprising when one considers the difference in net charge and electron energy between the two cases.

#### IV. CONCLUSIONS

We have performed distorted-wave, unitarized distorted-wave, and close-coupling calculations for the  $1s \rightarrow 2l$  transitions in  $\text{Li}^+$  in order to investigate the sensitivity of differential cross sections to the level of scatter-

ing approximation. The shape and magnitude of the differential cross section has been shown to be extremely sensitive to the level of continuum coupling included in the calculation. Thus it appears highly unlikely that the distorted-wave approximation will produce reliable differential excitation cross sections, at least for lower stages of ionization. This is true even when the total cross sections are in close agreement. Additional calculations will be needed to investigate how far this sensitivity will persist as a function of ionization stage.

As new generations of electron-ion collision experiments are developed, which produce differential cross sections with respect to scattering angle, or partial cross

sections over ranges of angles, we will surely have more severe tests of electron-ion scattering theory.

#### ACKNOWLEDGMENTS

We would like to thank Ron Henry, Gordon Dunn, and Ron Phaneuf for a number of very useful conversations. This work has supported by the Office of Fusion Energy, U.S. Department of Energy, under Contract No. DE-AC05-84OR21400 with Martin Marietta Energy Systems, Inc. and Contract No. DE-FG05-86ER53217 with Auburn University.

- 
- <sup>1</sup>W. C. Fon, K. A. Berrington, and A. E. Kingston, *J. Phys. B* **21**, 2961 (1988).
- <sup>2</sup>I. D. Williams, A. Chutjian, and R. J. Mawhorter, *J. Phys. B* **19**, 2189 (1986).
- <sup>3</sup>G. H. Dunn (private communication).
- <sup>4</sup>W. L. Wyngaarden, K. Bhadra, and Ronald J. W. Henry, *Phys. Rev. A* **20**, 1409 (1979).
- <sup>5</sup>Randy B. Christensen and David W. Norcross, *Phys. Rev. A* **31**, 142 (1985).
- <sup>6</sup>Wade T. Rogers, J. Ostgaard Olsen, and Gordon H. Dunn, *Phys. Rev. A* **18**, 1353 (1978).
- <sup>7</sup>Yukikazu Itikawa and Kazuhiro Sakimoto, *Phys. Rev. A* **38**, 664 (1988).
- <sup>8</sup>Kazuhiro Sakimoto and Yukikazu Itikawa, *Phys. Rev. A* **40**, 3646 (1989).
- <sup>9</sup>Stefano A. Salvini, *Comput. Phys. Commun.* **27**, 25 (1982).
- <sup>10</sup>C. Froese-Fischer, *Comput. Phys. Commun.* **14**, 145 (1978).
- <sup>11</sup>M. S. Pindzola, D. C. Griffin, and C. Bottcher, *Phys. Rev. A* **39**, 2385 (1989).
- <sup>12</sup>M. A. Crees, M. J. Seaton, and P. M. H. Wilson, *Comput. Phys. Commun.* **15**, 23 (1978).
- <sup>13</sup>This program is unpublished. Recent references are *Atoms in Astrophysics*, edited by P. G. Burke and W. Eissner (Plenum, New York, 1983); H. Nussbaumer and P. J. Storey, in *ibid.*
- <sup>14</sup>*Atomic Energy Levels and Grotrian Diagrams*, edited by S. Bashkin and J. O. Stoner, Jr. (North-Holland, Amsterdam, 1975), Vol. 1.
- <sup>15</sup>K. A. Berrington, W. C. Fon, and A. E. Kingston, *Mon. Not. R. Astron. Soc.* **200**, 347 (1982).
- <sup>16</sup>K. A. Berrington, P. G. Burke, L. C. G. Freitas, and A. E. Kingston, *J. Phys. B* **18**, 4135 (1985).
- <sup>17</sup>Keith A. Berrington and Arthur E. Kingston, *J. Phys. B* **20**, 6631 (1987).